Polymer 52 (2011) 4189–4198

Contents lists available at ScienceDirect

Polymer

journal homepage: www.elsevier.com/locate/polymer

Fumed silica filled poly(dimethylsiloxane-urea) segmented copolymers: Preparation and properties

Emel Yilgor [a], Tugba Eynur [a], Cagla Kosak [a], Sevilay Bilgin [a], Iskender Yilgor [a,*], Ozge Malay [b], Yusuf Menceloglu [b], Garth L. Wilkes [c]

[a] Surface Science and Technology Center, Chemistry Department, Koc University, Sariyer 34450, Istanbul, Turkey
[b] Advanced Composites and Polymer Processing Laboratory, Faculty of Engineering and Natural Sciences, Sabanci University, Tuzla 34956, Istanbul, Turkey
[c] Department of Chemical Engineering, Virginia Tech, Blacksburg, VA 24061-0211, USA

ARTICLE INFO

Article history:
Received 8 April 2011
Received in revised form
22 July 2011
Accepted 26 July 2011
Available online 30 July 2011

Keywords:
Fumed silica
Silicone copolymer
Nanocomposite

ABSTRACT

Novel fumed silica filled thermoplastic poly(dimethylsiloxane-urea) (TPSU) segmented copolymers were synthesized and characterized. TPSU copolymers were prepared from a cycloaliphatic diisocyanate, aminopropyl terminated PDMS oligomers with number average molecular weights of 3,200, 10,800 and 31,500 g/mol and 2-methyl-1,5-diaminopentane chain extender. Two different types of fumed silica HDK H2000 (hydrophobic) and HDK N20 (hydrophilic) were utilized and incorporated into silicone-urea copolymers in amounts of 1–60% by weight. Influence of the silica type (hydrophilic versus hydrophobic), amount of silica loading and the PDMS soft segment molecular weight on the morphology, tensile properties and modulus-temperature behavior of the nanocomposites were determined. Major observations of this study were: (i) under the blending conditions used, incorporation of silica does not seem to interfere significantly with the hydrogen bonding between urea groups, (ii) incorporation of silica does not affect the glass transition temperature of PDMS, (iii) incorporation of silica influences the tensile and thermomechanical properties of silicone-urea segmented copolymers significantly, (iv) average molecular weight of the PDMS soft segment in the silicone-urea copolymer plays a critical role on the improvement of the tensile properties of the fumed silica/TPSU composites.

1. Introduction

Polymeric composites and recently nanocomposites have received widespread attention due to the dramatic improvements in the performance of polymers through the incorporation of micro and nano sized fillers. Some of the important classes of nanoparticles used as fillers in polymeric composites include fumed silica, organoclays, carbon nanofibers, carbon nanotubes, polyhedral oligomeric silsesquioxanes, titanium oxide and very recently graphene [1–5]. Many polymers have been used as hosts for the preparation of composites based on such fillers [1–5]. Such composites have in general displayed highly improved thermal, mechanical and engineering properties when compared with their virgin resins.

Silicone (polydimethylsiloxane) (PDMS) elastomers display a unique combination of properties, such as; a very low glass transition temperature, low surface energy, hydrophobicity, high gas permeability, excellent thermal and oxidative stability and biocompatibility and find many commercial applications as sealants, adhesives, membranes and elastomers in automotive and construction industries, microelectronics, specialty textiles, medical devices and implants [6]. They are oxidatively and thermally stable in a very wide temperature range of −100 to +300 °C. Unfortunately, due to very weak intermolecular forces and high chain flexibility silicone elastomers generally display poor ambient and high temperature mechanical properties relative to many conventional elastomeric materials of higher glass transition. As a result for any application that requires mechanical strength silicone elastomers are always filled with substantial amounts of fumed silica (up to 40–60% by weight) to improve their mechanical properties [6,7]. Interestingly, silica filled silicone elastomers are some of the first examples of nanocomposites that have displayed a wide range of commercial applications.

Recently, we demonstrated the synthesis and characterization of thermoplastic poly(dimethylsiloxane-urea) segmented copolymers (TPSU), which displayed thermal and mechanical properties similar or superior to that of crosslinked silicone elastomers without the need to use any fillers [8–10]. These TPSU copolymers are obtained by the chemical combination of extremely non-polar and weak PDMS oligomers with extremely polar and very

* Corresponding author. Tel.: +90 212 338 1418; fax: +90 212 338 1599.
E-mail address: iyilgor@ku.edu.tr (I. Yilgor).

0032-3861/$ – see front matter © 2011 Elsevier Ltd. All rights reserved.
doi:10.1016/j.polymer.2011.07.041

strongly hydrogen bonded urea segments. Due to major differences between the solubility parameters of PDMS and urea groups, TPSU copolymers display microphase separation even at very low urea contents. We also recently reported the effect of PDMS soft segment length on the mechanical properties of TPSU copolymers with low urea hard segment contents of 2–15% by weight [11,12].Thermal and mechanical properties of TPSU are mainly determined by the hydrogen bonding between the urea groups and therefore it is directly related to the hard segment content of the copolymer [8–10]. Strongly hydrogen bonded urea groups in localized regions/domains act as both physical crosslinks and "pseudo" reinforcing fillers in TPSU. As a result, in general it may be considered that TPSU copolymers do not need to be filled with silica or other fillers to improve their mechanical properties. It may even be anticipated that incorporation of silica fillers would interfere with the strong hydrogen bonding within the urea hard segments and weaken them and as a result might even negatively influence the mechanical properties of such silicone-urea copolymers. To our knowledge there are no reports in the open literature which discusses the use of reinforcing silica fillers for silicone-urea segmented elastomers. This study was undertaken to determine if silica fillers play a synergistic effect in improving the mechanical properties of thermoplastic silicone-urea copolymers with low hard segment contents, similar to those of silicone elastomers. Furthermore we also wanted to investigate how the fillers influenced the hydrogen bonding in the segmented silicone copolymers.

In this paper we report initial results of our studies, where TPSU copolymers based on PDMS soft segments with molecular weights $<M_n>$ of 3,200, 11,000 and 32,000 g/mol and fairly low urea hard segment contents of 5–8% by weight were reinforced with hydrophobic or hydrophilic fumed silica. Thermal and mechanical properties of novel TPSU/silica (nano)composites with silica loadings of 1–60% by weight were determined. The effect of; (i) silica type, (ii) amount of silica loading and (iii) the PDMS soft segment molecular weight in the copolymer on thermal and mechanical properties of the resultant thermoplastic composites were investigated.

2. Experimental

2.1. Materials

α,ω-Aminopropyl terminated polydimethylsiloxane (PDMS) oligomers with $<M_n>$ values of 3,200, 10,800 and 31,500 g/mol and fumed silica samples HDK N20 (hydrophilic) and HDK H2000 (hydrophobic) were kindly supplied by Wacker Chemie, Munich, Germany. Primary particle size for both fumed silica type is reported to be 5–30 nm, which increases to 100–250 nm after aggregation. Hydrophilic silica (N20) is produced by the hydrolysis of chlorosilanes in an oxyhydrogen flame [13]. It consists of >99.8% by weight of amorphous silicon dioxide and has a silanol content of 2SiOH/nm^2. Hydrophobic silica (H2000) is obtained by the reaction of hydrophilic silica with trimethyl chlorosilane or hexamethyldisilazane producing a surface having a rich content of hydrophobic trimethylsiloxy groups [13]. The specific surface area for both materials is reported to be 170–230 m^2/g. Cycloaliphatic diisocyanate bis(4-isocyanatocyclohexyl)methane (HMDI) was kindly supplied by Bayer, Germany, which had a purity better than 99.5%. The chain extender 2-methyl-1,5-diaminopentane (Dytek A, DY) was provided by DuPont. Reagent grade 1,3-dimethylurea (DMU), isopropyl alcohol (IPA) and tetrahydrofuran (THF) were obtained from Merck and were used as received.

2.2. Syntheses of PDMS-urea copolymers

Polymerization reactions were carried out in three-neck, round bottom, Pyrex reaction flasks equipped with an overhead stirrer and an addition funnel. All reactions were carried out in THF/IPA (50/50 by volume) solution, at room temperature using the "prepolymer" method. A detailed description of the polymerization reactions is provided in earlier publications [8–11].

2.3. Preparation of filled systems

Fumed silica filled/TPSU materials were prepared by dissolving silicone-urea copolymers in THF (about 12–15% solids by weight) and then adding the fumed silica filler and stirring the system on a magnetic stirrer with a speed of 50 rpm overnight until a homogeneous distribution of the filler is obtained. The mixture was then subjected to an ultrasonic treatment at a frequency of 35 kHz on a Sonorex RK 255H type ultrasonic bath (Bandelin, Berlin, Germany) for 60 min. To obtain thin films (0.3–0.5 mm) the solutions were cast into Teflon molds and the solvent was evaporated at room temperature. Final drying was obtained in an air oven at 60 °C, until constant weight was reached. When hydrophilic silica (N20) was used as the filler in amounts over 20% by weight, it was somewhat difficult to obtain homogeneous solutions. Therefore, most of our efforts were concentrated on the filled materials prepared by using the hydrophobic silica (HDK H2000).

2.4. Characterization methods

FTIR spectra were recorded on a Nicolet 7600 FTIR spectrometer using solution cast films on KBr discs. 20 Scans were taken for each spectrum with a resolution of 2 cm^{-1}. Gel permeation chromatography (GPC) studies were performed on a Shimadzu LC20-A system equipped with an 8 × 50 mm precolumn and 50, 10^2, 10^3, 10^4, and 10^5 Å SDV columns (from Polymer Standards Service) and a refractive index detector. Measurements were made in a THF solution at 30 °C, with a flow rate of 1.0 mL/min. Polystyrene standards with $<M_n>$ values in 1000–1,000,000 g/mol were used for calibration. Dynamic mechanical analysis of the samples was obtained on a TA DMA Q800 instrument. Measurements were made in tensile mode at 1 Hz, between −150 and 280 °C, under a nitrogen atmosphere and at a heating rate of 3 °C/min. Morphologies of composite films were examined using a field-emission scanning electron microscope (FE-SEM) (SUPRA 35VP, LEO, Germany) operated at 2 kV. The films were fractured in liquid nitrogen and the fracture surfaces (cross-section) were coated with a thin layer of carbon prior to SEM examinations. AFM characterization was performed using a Nanoscope III Atomic Force Microscope (Digital Instruments, Santa Barbara, CA USA) using the tapping mode with silicon cantilevers with a spring constant of typically 35–47.2 N/m (OMCL-AC160TS, Olympus, Japan, typical drive frequency of 303 kHz). Fumed silica/TPSU composite films dip-coated on freshly cleaved mica were used to perform AFM analyses to further investigate the shape and distribution of fumed silica in the composites. AFM images were obtained on the free or air surface of the films and were processed using the WSxM software package. Stress-strain tests were performed on an Instron model 4411 tester. Dog-bone shaped specimens (ASTM D 1708) were punched out of the films. Length and width of dog-bone specimens were 38.0 and 4.75 mm respectively. Film thicknesses were in the range of 0.4–0.6 mm. Tensile tests were performed with a crosshead speed of 25.00 mm/min (L_o = 24.0 mm). Tests were conducted at room temperature and for each polymer at least three specimens were tested.

3. Results and discussion

As stated earlier, this study was undertaken in order to understand the effect of fumed silica incorporation on the tensile properties and thermomechanical behavior of thermoplastic,

Table 1
Chemical composition and average molecular weights of the silicone-urea copolymers (*) Molar ratio of [PDMS]/[HMDI]/[CE]. (**) Obtained from reaction stoichiometry. (***) Obtained from GPC.

Sample	PDMS $<M_n>$ (g/mol)	Chain Extender (CE)	Molar Ratio (*)	Hard segment (wt%) (**)	$<M_n>$ (g/mol) (***)	$<M_w>$ (g/mol) (***)
PSU-3.2-7.6	3200	–	1/1/0	7.57	4.6×10^4	8.2×10^4
PSU-11-DY-5.6	10,800	DY	1/2/1	5.56	2.6×10^5	3.8×10^5
PSU-32-DY-5.3	31,500	DY	1/5/4	5.34	3.9×10^5	6.3×10^5

segmented poly(dimethylsiloxane-urea) (TPSU) copolymers with fairly low urea hard segment contents. The variables investigated were; (i) type of silica used (hydrophobic versus hydrophilic), (ii) amount of silica loading in the copolymers, and (iii) the PDMS soft segment molecular weight of the copolymer. Table 1 gives a list of TPSU copolymers used in this study and provides information on their chemical compositions and average molecular weights. Codes used to identify the copolymers were as follows: PSU indicates the silicone-urea copolymer; the following number indicates the $<M_n>$ value of PDMS in kg/mole; which is followed by two letters (DY) indicating that the chain extender was used. The final numbers indicate the urea hard segment content of the copolymer in weight percent. For example, a PDMS-10,800, HMDI and DY based silicone-urea copolymer with 5.56% by weight hard segment content is coded as: PSU-11-DY-5.6. In contrast, PSU-3.2-7.6 was prepared using stoichiometric amounts of PDMS-3200 and HMDI, without a chain extender. Table 2 provides the list of silica/TPSU composites and their compositions prepared and used in this study.

Two types of fumed silica from Wacker Chemie, hydrophobic (HDK H2000) and hydrophilic (HDK N20) were employed in the preparation of composites. In the nomenclature (H) or (N) indicates H2000 and N20 silica respectively and the numbers show the amount of silica in the TPSU copolymer in weight percent [(weight silica/weight copolymer)×100]. Silica content is provided both as weight percent and volume percent [(volume silica/volume copolymer)×100] in Table 2. Bulk densities of TPSU and silica were taken as 1.0 and 2.2 g/cm^3 respectively.

3.1. FTIR studies

FTIR spectroscopy was applied in order to understand the presence and nature of possible interactions between the silica fillers and silicone-urea copolymers. FTIR is a simple but very sensitive technique to investigate the nature and extent of hydrogen bonding in the polyureas copolymers especially by examining the peak shifts in the carbonyl region (1800–1450 cm^{-1}) [14]. For FTIR studies very thin films (ca. 50 μm) were cast onto KBr discs from THF/IPA solution and the solvent was evaporated using an air gun. Spectra were obtained with a resolution of 2 cm^{-1}.

Table 2
Compositions of fumed silica/TPSU composites investigated.

Sample	PDMS $<M_n>$ g/mol	Silica content		
		Type	Weight % (wt silica/ wt polymer)	Volume % (vol silica/ vol polymer)
PSU-3.2-7.6	3200	–	–	–
PSU-3.2-7.6-H-01	3200	H	1	0.45
PSU-3.2-7.6-H-05	3200	H	5	2.3
PSU-3.2-7.6-H-10	3200	H	10	4.5
PSU-3.2-7.6-H-15	3200	H	15	6.8
PSU-3.2-7.6-H-20	3200	H	20	9.1
PSU-3.2-7.6-H-25	3200	H	25	11.4
PSU-3.2-7.6-H-40	3200	H	40	18.2
PSU-3.2-7.6-N-01	3200	N	1	0.45
PSU-3.2-7.6-N-05	3200	N	5	2.3
PSU-3.2-7.6-N-10	3200	N	10	4.5
PSU-3.2-7.6-N-20	3200	N	20	9.1
PSU-11-DY-5.6	10,800	–	–	–
PSU-11-DY-5.6-H-10	10,800	H	10	4.5
PSU-11-DY-5.6-H-20	10,800	H	20	9.1
PSU-11-DY-5.6-H-40	10,800	H	40	18.2
PSU-32-DY-5.3	31,500	–	–	–
PSU-32-DY-5.3-H-20	31,500	H	20	9.1
PSU-32-DY-5.3-H-40	31,500	H	40	18.2
PSU-32-DY-5.3-H-60	31,500	H	60	27.3

3.1.1. FTIR studies on model dimethylurea and fumed silica blends

1,3-Dimethylurea (DMU) is a very useful model compound to mimic the hard segments in silicone-urea copolymers. To investigate the presence of interactions between silica and the urea groups we prepared 10% by weight silica containing DMU blends designated respectively as DMU-H-10 and DMU-N-10 in THF, cast them on KBr discs and obtained their transmission FTIR spectra. The carbonyl region of the FTIR spectra for DMU and its blends with silica are reproduced in Fig. 1. DMU shows a strongly hydrogen bonded C=O peak centered at 1624 cm^{-1} and two well defined shoulders at 1585 (amide II, stretching) and 1537 cm^{-1} (amide II, vibration). As can be seen in Fig. 1, FTIR spectra of DMU-H-10 and DMU-N-10 overlap completely and are also identical to that of DMU. Results of the FTIR studies do not indicate any significant change in the nature of the hydrogen bonded carbonyl groups in dimethylurea as a result of silica incorporation.

3.1.2. FTIR studies in silica filled TPSU

We were mainly interested in finding out if any specific interactions take place between; strongly hydrogen bonded urea hard segments and silica particles and Si—O—Si linkages in the PDMS backbone and the silica particles. For this purpose we closely examined the N—H region (3400-3300 cm^{-1}) and the C=O region (1800-1500 cm^{-1}) together with the Si—O—Si region (1000–1100 cm^{-1}). Fig. 2-(a) provides the comparative FTIR spectra of PSU-3.2-7.6, PSU-3.2-7.6-H-20 and PSU-3.2-7.6-N20 in 3500–2800 cm^{-1} range which covers the N—H and C—H stretching regions. Interestingly, at ambient temperature, there is no noticeable difference in the locations of the stretching frequencies or the general magnitudes of the absorptions between

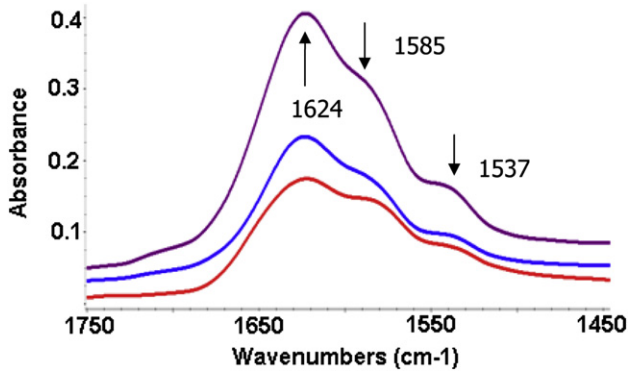

Fig. 1. FTIR spectra of DMU (bottom) and its blends with 10% by weight hydrophobic (DMU-H-10) (middle) and hydrophilic (DMU-N-10) (top) silica.

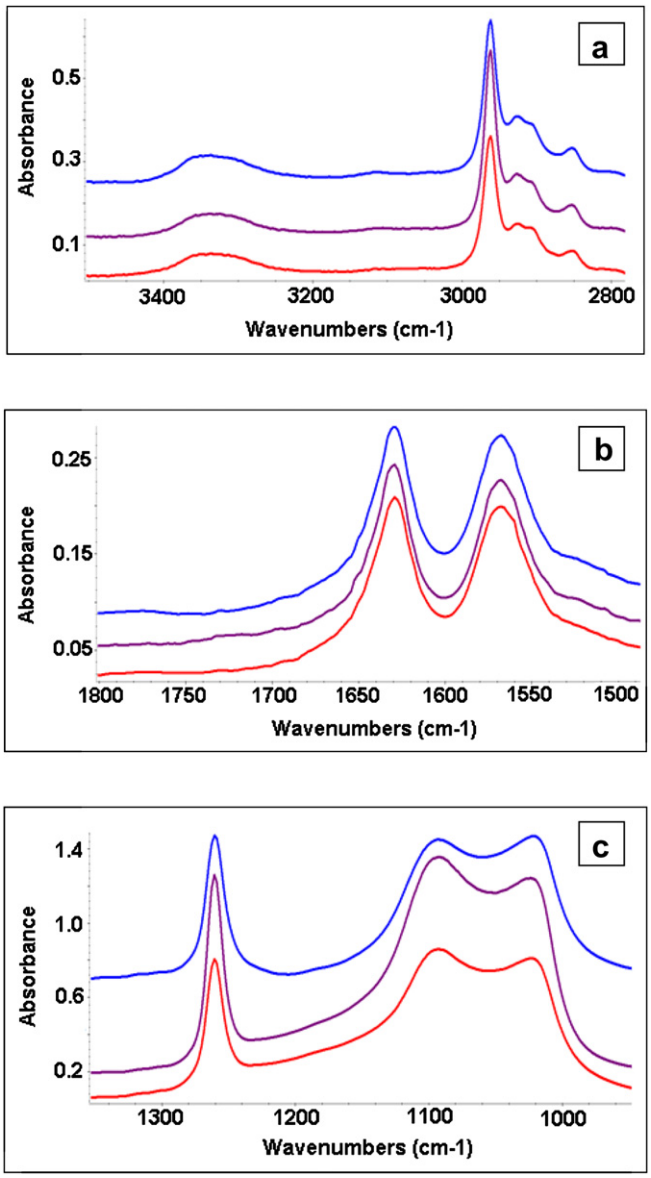

Fig. 2. (a) 3500–2800 cm^{-1} (b) 1800–1500 cm^{-1} and (c) 1350–950 cm^{-1} region of the FTIR spectra for PSU-3.2-7.6 (top), PSU-3.2-7.6-H-20 (middle) and PSU-3.2-7.6-N20 (bottom).

the spectra for the virgin polymer and polymer composites. All samples show broad and symmetrical N—H peaks in the 3400–3250 cm^{-1} range and completely overlapping C—H peaks below 3000 cm^{-1}. Fig. 2-(b) shows the carbonyl region of the FTIR spectra (1800–1500 cm^{-1}) for PSU-3.2-7.6, PSU-3.2-7.6-H-20 and PSU-3.2-7.6-N20. In this region we again observe almost identical spectra for all samples, which display two very strong and symmetrical peaks. The first peak is centered at 1630 cm^{-1} indicating strongly hydrogen bonded C=O stretching and the other is centered at 1568 cm^{-1} due to amide II (HN—C=O) stretching. When closely examined, a weak and broad almost shoulder-like peak is also observed in the 1750–1720 cm^{-1} range for PSU-3.2-7.6-H-20 sample, which indicates the presence of some free or non hydrogen bonded C=O groups. This is most probably due to the interference of the hydrophobic silica (H2000) with the strongly hydrogen bonded urea groups in the copolymer resulting in a slight break-up of the hydrogen bonded structure of the hard segments. Such a behavior is not observed for the hydrophilic silica filled PSU-3.2-7.6-N20. This may be due to the fact that even if N20 interacts with the urea groups (which is most probably the case), due to the presence of O—H groups on its surface it can also form strong hydrogen bonding with the urea groups, thus resulting in no net change in the hydrogen bonded structure of the system.

Fig. 2-(c) provides the FTIR spectra in the 1350–950 cm^{-1} region. Similar to the observations made in Fig. 2-(a) and (b) there is no significant change in the Si—O—Si doublet of the PDMS backbone at 1093 and 1024 cm^{-1}. Slight broadening of the doublet for the filled systems is due to the absorption of the fumed silica in this region. The sharp and symmetrical peak centered at 1260 cm^{-1} region is due to the $—CH_3$ bending mode in PDMS, which is identical for all three samples. This also indicates the absence of a strong interaction between silica and PDMS.

3.2. SEM studies on the morphology of the composites

Morphology of the fumed silica/poly(dimethylsiloxane-urea) composites were studied by scanning electron microscopy (SEM). SEM studies are useful in providing direct information on the effectiveness of the sample preparation procedure employed in obtaining a homogeneous random distribution of the silica particles in the nanocomposites. SEM pictures also provide quantitative information on the geometry and the size of the silica domains in the TPSU matrix. Since composite films were prepared by solution casting, one important question is whether there is sedimentation of the particles during solvent evaporation leading to an uneven distribution of particles in the polymeric composite. To answer this question we obtained SEM images of PSU-11-DY-5.6-H-20 sample from the cross-section (top, middle and bottom portion) of the fractured surfaces. These images, which indicate a homogeneous distribution of silica particles throughout the composite film, are provided in Fig. 3. In addition to SEM, we also performed dynamic light scattering measurements on silica/silicone-urea solutions to find out if any agglomeration took place over time, for up to 5 days. The results also indicated no change in the particle size distribution in the solutions over time.

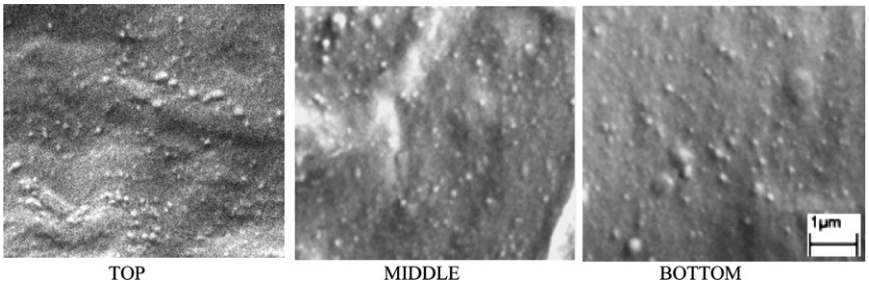

Fig. 3. SEM images of PSU-11-DY-5.6-H-20 sample from the top, middle and bottom portion of the cross-section of a fractured surface after cooling in liquid nitrogen.

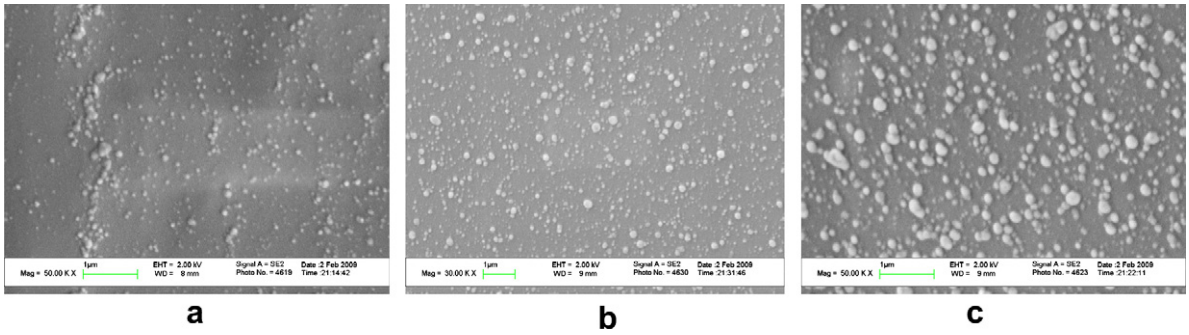

Fig. 4. SEM pictures for PSU-3.2-7.6 based composites containing hydrophobic silica H2000. (a) PSU-3.2-7.6-H-05, (b) PSU-3.2-7.6-H-15, (c) PSU-3.2-7.6-H-25.

SEM pictures for PSU-3.2-7.6 and hydrophobic silica (H2000) containing composites with 5, 15 and 25% by weight of silica are reproduced in Fig. 4-(a)–(c). As can clearly be seen in Fig. 4-(a)–(c), distribution of silica in the TPSU matrix is fairly spherical at all concentrations. However as the silica concentration increases the particle size also increases and the distribution seem to become somewhat broader.

In the PSU-3.2-7.6-H-05 composite, the silica particle size distribution is fairly homogeneous where the particle size is in 50–100 nm range. On the other hand in PSU-3.2-7.6-H-15 the silica particle sizes become larger (50–200 nm) and the distribution becomes slightly broader. In PSU-3.2-7.6-H-25, where silica concentration becomes fairly high, although the distribution of silica particles is fairly homogeneous, many of the particles seems to be slightly distorted from a spherical shape. The average particle size is in 100–250 nm range. In summary, SEM results clearly show a homogeneous distribution of spherical silica particles in the PSU-3.2-7.6 matrix, where the average particle size increases with silica content, which may be an expected behavior for samples prepared by the solution method we have utilized.

Fig. 5-(a)–(d) provide SEM pictures for PDMS-10,800 based silicone-urea copolymer, PSU-11-DY-5.6 and its composites containing 10, 20 and 40% by weight of H2000. The SEM micrograph of the virgin copolymer (Fig. 5-(a) displays a very smooth surface, which is expected. As reproduced in Fig. 5-(b) and (c), SEM micrographs of PSU-11-DY-5.6-H-10 and PSU-11-DY-5.6-H-20 show a fairly homogeneous distribution of spherical silica particles in the TPSU matrix where particle sizes are in the range of 50–200 nm for both samples. As the amount of filler is increased to 40% by weight (PSU-11-DY-5.6-H-40) SEM shows a dramatic change in the particle geometry, size and distribution. As can be seen in Fig. 5-(d) although most of the silica particles are spherical with particle sizes in the range of 50–200 nm as in the other samples containing 10 and 20% H2000, the micrographs also reveal there are some much larger globular-like particles.

Tapping mode AFM phase images of 20 and 40% H2000 containing PSU-11-DY-5.6 based composites are provided in Fig. 6. We were not successful in obtaining any characteristic feature in our AFM studies on the phase image of virgin PSU-11-DY-5.6. This is most probably due to very low hard segment content of the copolymer, together with the complete surface coverage of PSU by PDMS, which is well known. On the other hand as shown in Fig. 6-(a) and (b), silica particles are well distributed in the composites. In line with SEM observations, AFM studies also reveal substantial change in the shape and size of the particles with an increase in the amount of silica filler. For 20% loading, particles could retain their spherical shape even though they are closely spaced. However, at 40% loading, clusters of spherical particles form globular and larger

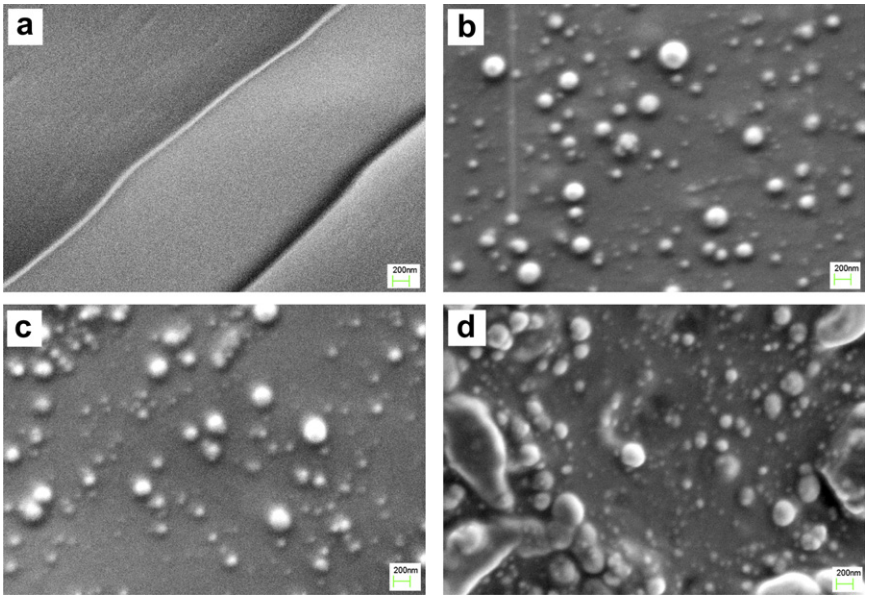

Fig. 5. SEM pictures for PSU-11-DY-5.6 based nanocomposites containing hydrophobic silica H2000. (a) PSU-11-DY-5.6, (b) PSU-11-DY-5.6-H-10, (c) PSU-11-DY-5.6-H-20, (d) PSU-11-DY-5.6-H-40.

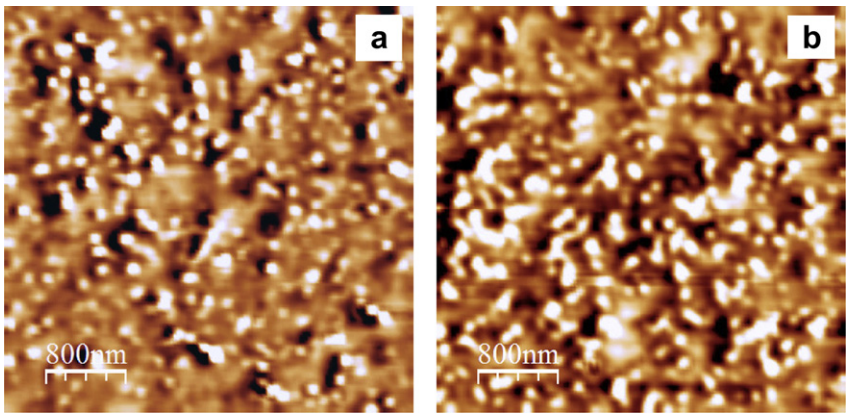

Fig. 6. Tapping Mode AFM phase images of air surfaces of PSU-11-DY-5.6 based nanocomposites containing hydrophobic silica H2000 (films were dip-coated on mica surface). (a) PSU-11-DY-5.6-H-20 and (b) PSU-11-DY-5.6-H-40.

particles as a result of agglomeration. The root-mean square roughness (R_q) of the unfilled polymer (PSU-11-DY-5.6) was 0.6 nm, whereas 20 and 40 wt% hydrophobic silica (H2000) filled composite films (PSU-11-DY-5.6-H-20 and PSU-11-DY-5.6-H-40) both had an R_q value of approximately 3 nm.

3.3. Thermomechanical analysis

Incorporation of fumed silica fillers are expected to dramatically influence the modulus-temperature profiles of silicone-urea copolymers, especially in the rubbery plateau region. Comparative modulus-temperature and tan delta-temperature curves for PSU-3.2-7.6 and two composites containing 20% by weight of H2000 (PSU-3.2-7.6-H-20) and N20 (PSU-3.2-7.6-N20) are reproduced on Fig. 7-(a). For better resolution, the tan delta-temperature curves for the PDMS glass transition region are reproduced in Fig. 7-(b).

As can be seen in Fig. 7-(a), regardless of the silica type used its incorporation does not greatly influence the glass transition temperature (Tg) of the copolymer. Interestingly, unfilled or silica filled samples do not display PDMS crystallization and melting, which is believed due to somewhat low molecular weight of the PDMS segment in the copolymer. PDMS crystallization is typically observed when PDMS segment molecular weight is ca. 7000 g/mol or higher [15–18]. As can be seen in Fig. 7-(b) and provided on Table 3, Tg value of PSU-3.2-7.6 is —114 °C, slightly higher than the value of −120 °C usually obtained by differential scanning calorimetry (DSC). Such a small difference in Tg obtained by the DMA vs DSC is expected.

As tabulated on Table 3, only a slight difference between the Tg values (obtained from the peak points of tan delta curves) of the unfilled (−114 °C) and filled (−112 °C) silicone-urea copolymer also indicates that silica fillers do not interact strongly with the PDMS backbone or do not influence the chain flexibility. Secondly, the glassy modulus of the composites (at −150 °C) shows a modest increase from 4.00 MPa to above 5.00 MPa with the incorporation of silica. Hydrophilic N20 seems to provide a slightly higher glassy modulus than the hydrophobic H2000 filler for the composite at 20% loading. The most dramatic influence of silica incorporation is observed on the rubbery plateau of the composites. The type of the silica used also makes a major difference in the properties of the rubbery plateau.As can be seen in Fig. 7, PSU-3.2-7.6 displays a fairly sharp glass transition region between −120 and −100 °C, followed by a well defined rubbery plateau region from −100 to about +25 °C. As the temperature is increased, especially above 100 °C, hydrogen bonding between urea groups begins to weaken and as a result thermoplastic PSU-3.2-7.6 shows rubbery and viscous flow below 150 °C. In contrast, incorporation of 20% by weight of H2000 increases the rubbery plateau modulus (at 25 °C) substantially from 5.0 kPa to 25.0 kPa and extends the rubbery plateau and flow to slightly higher temperatures than the previous material. Interestingly, when 20% by weight of hydrophilic N20 is used as the filler, the rubbery plateau modulus increases further to 42.0 kPa, but most importantly the rubbery plateau is extended dramatically to beyond

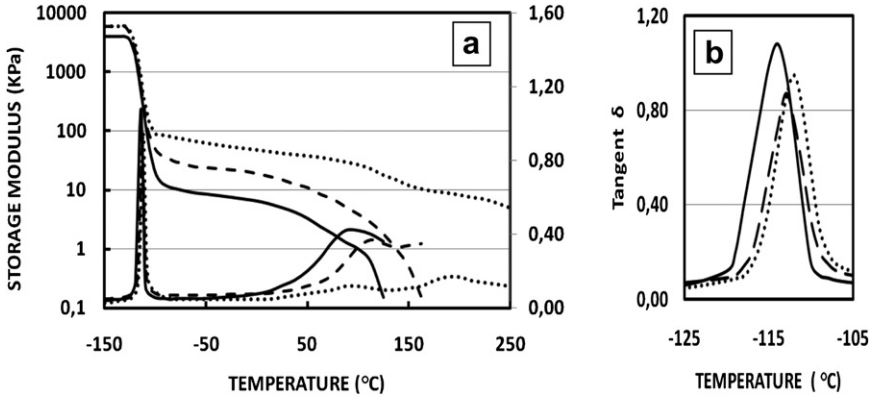

Fig. 7. Storage modulus-temperature and tan δ-temperature curves of PSU-3.2-7.6 (———), PSU-3.2-7.6-H-20 (— — —) and PSU-3.2-7.6-N20 (••••••••).

Table 3
Summary of DMA results for PSU-3.2-7.6 and composites.

Sample	Tg (°C)	Glassy modulus (MPa)	Rubbery plateau modulus at 25 °C (KPa)
PSU-3.2-7.6	−114	4.00	5.0
PSU-3.2-7.6-H-20	−113	5.20	25.0
PSU-3.2-7.6-N-20	−112	5.40	42.0

Table 4
Tensile properties of poly(dimethylsiloxane-urea) copolymers.

Polymer Code	HS Content (wt %)	Modulus (MPa)	Tens Str (MPa)	Elong. (%)
PSU-3.2-7.6	7.57	4.00	5.50	580
PSU-11-DY-5.6	5.56	1.20	1.65	280
PSU-32-DY-5.3	5.14	0.90	2.10	400

250 °C, which is above where thermal degradation temperature of the urea linkages would begin [19]. A summary of the results obtained from DMA curves (Tg, modulus values for the glassy and rubbery plateau regions) are provided on Table 3. Tg values are obtained from the tan delta-temperature curves.

Storage modulus-temperature curves for the higher molecular weight soft segment material PSU-32-DY-5.3 and PSU-32-DY-5.3-H-40 are reproduced in Fig. 8. As can clearly be seen in Fig. 8, incorporation of silica results in a substantial increase in the modulus of the glassy state from 2 MPa for the virgin (unfilled) polymer to about 6 MPa for the composite sample, an expected behavior from the presence of the reinforcing fillers in addition to some crystallization of the PDMS segments due to their higher molecular weight.

Both samples still show a well defined PDMS glass transition around −120 °C followed by a sharp PDMS melting transition around −50 °C, typical for semi-crystalline PDMS, which was not observed in PSU-3.2-7.6 due to its much lower PDMS molecular weight. Interestingly, these results indicate that the presence of 40% by weight of hydrophobic silica does not influence the crystallization behavior or crystallinity of PDMS-31,500 present in the polymer backbone. The PDMS melting transition at about −50 °C is followed by a fairly long rubbery plateau extending from −40 to +200 °C. The rubbery plateau of the virgin copolymer, which contains 94.7% by weight of PDMS is fairly flat in this region and shows only a slight drop around 200 °C. This clearly demonstrates the power of the hydrogen bonding in the system even with very low urea hard segment content. In contrast the rubbery plateau of 40% hydrophobic silica filled composite initially has a much higher modulus value compared to the virgin copolymer (PSU-32-DY-5.3) however, as temperature increases the rubbery modulus decreases slightly. This may indirectly indicate some interaction between the urea groups and the hydrophobic silica particles at these higher temperatures, somewhat reducing the strength of the hydrogen bonded structure of urea hard segments. Recall from Fig. 2-(b) that the ambient temperature FTIR results did not show major sign of and major difference in filler-matrix interactions nor does the DMA data suggest otherwise as well at ambient conditions.

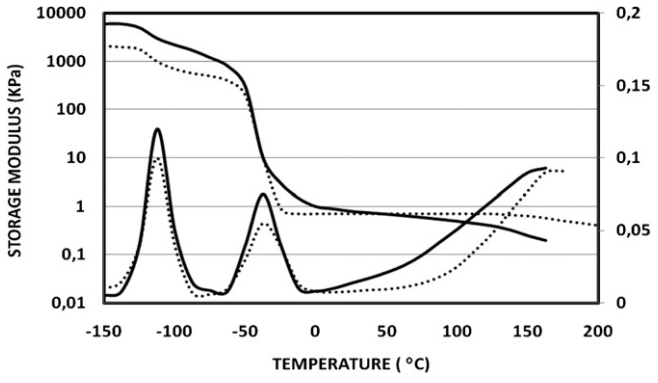

Fig. 8. Storage modulus-temperature and tan δ-temperature curves for PSU-32-DY-5.3 (••••••••) and PSU-32-DY-5.3-H-40 (———).

3.4. Stress-strain behavior

One of the major aims of incorporating silica fillers into silicone elastomers is to improve the mechanical properties of the final elastomer [6,7]. Thermoplastic silicone-urea copolymers inherently display good mechanical properties due to microphase separation and strong hydrogen bonding between urea hard segments [9,10]. Nevertheless we wanted to investigate the effect of silica incorporation into silicone-urea copolymers, hoping that there would be a synergistic effect on the mechanical properties. Table 4 provides the data on the stress–strain properties of the three unfilled TPSU copolymers utilized in this study. As can clearly be seen from this Table, due to their low urea hard segment contents, Young's modulus and tensile strengths of these copolymers are in the range of 0.90–4.00 MPa and 1.65 to 5.50 MPa respectively, depending on their chemical composition.

Stress-strain curves for the virgin PSU-3.2-7.6 and silica composites containing 1–25% by weight of hydrophobic silica (H2000) are reproduced in Fig. 9.

As can be seen from these curves, Young's modulus and the ultimate tensile strength of the composites display a gradual increase as a function of the amount of silica incorporation, whereas a gradual decrease in the elongation at break values, which becomes somewhat significant at higher silica loadings, is also observed. Stress-strain tests were also carried out for the composite materials based on PSU-3.2-7.6 and hydrophilic silica N20. These stress-strain curves are not shown (except for PSU-3.2-7.6-N20 in Fig. 10) since they followed a similar trend as those in Fig. 8, but the results are reported in Table 5.

Table 5 summarizes the results obtained on the tensile properties of PSU-3.2-7.6 and its composites based on hydrophobic (H2000) and hydrophilic (N20) silica. As can be seen from the data provided for those samples containing equal amounts of silica fillers, improvement in the moduli and ultimate tensile strengths of composites based on hydrophilic silica N20 is slightly higher than those based on hydrophobic silica, H2000. On the other hand

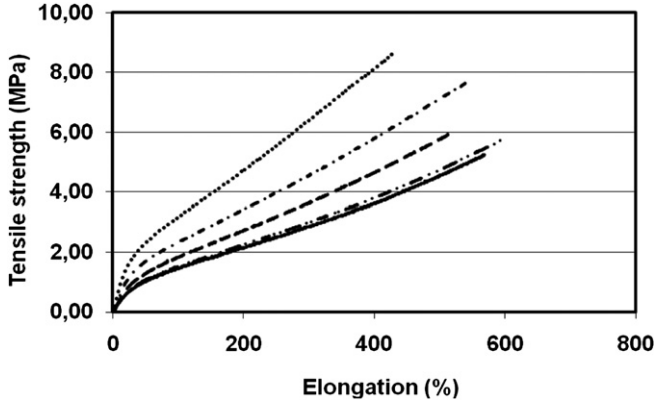

Fig. 9. Stress-strain curves for PSU-3.2-7.6 and composites based on H2000. PSU-3.2-7.6 (———), PSU-3.2-7.6-H-1 (— •• —), PSU-3.2-7.6-H-5 (— — —), PSU-3.2-7.6-H-15 (— • — • —) and PSU-3.2-7.6-H-25 (••••••••).

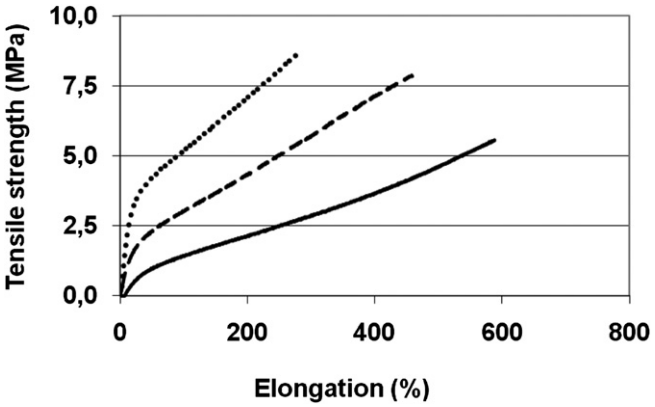

Fig. 10. Stress-strain curves for PSU-3.2-7.6 (———), PSU-3.2-7.6-H-20 (— — —) and PSU-3.2-7.6-N20 (••••••••).

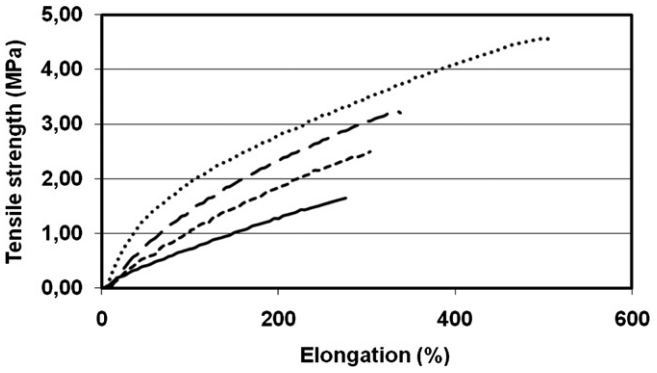

Fig. 11. Stress-strain curves for PSU-11-DY-5.6 and composites based on H2000. PSU-11-DY-5.6 (———), PSU-11-DY-5.6-H-10 (- - - -), PSU-11-DY-5.6-H-20 (— — —), and PSU-11-DY-5.6-H-40 (••••••••)

elongation at break values of N20 filled TPSU composites are significantly lower.

In order to provide a better comparison on the effect of silica type on the tensile behavior of PSU-3.2-7.6 composites, comparative stress-strain curves for PSU-3.2-7.6 (unfilled), PSU-3.2-7.6-H-20 and PSU-3.2-7.6-N20 are reproduced in Fig. 10.

Very interestingly the influence of silica incorporation on the tensile properties of silicone-urea copolymers based on higher molecular weight soft segments, namely PDMS-10,800 and PDMS-31,500 was even much more dramatic. Fig. 11 provides the stress-strain curves for PSU-11-DY-5.6 and its composites based on H2000, containing 10, 20 and 40% by weight of silica.

Unlike composite materials prepared from PSU-3.2-7.6 based on somewhat lower molecular weight PDMS-3200, which showed improvement in modulus and ultimate tensile strength, but a decrease in elongation at break values, composites based on PDMS-10,800 display an increase in all properties, including substantial improvement in the values of elongation at break. As discussed below, similar behavior is also observed for PDMS-31,500 based silicone-urea composites. A summary of the results obtained on the tensile properties of PSU-11-DY-5.6 and its composites as a function of silica content is provided on Table 6.

Fig. 12 provides the stress-strain curves for PSU-32-DY-5.3 and its composites based on H2000, containing 20 and 40% hydrophobic silica H2000. Similar to observations made for PSU-11-DY-5.6 based systems, significant increases in every tensile property (Young's modulus, ultimate tensile strength and elongation at break) are also observed for PSU-32-DY-5.3 composites. A summary of the tensile test results for PDMS-31,500 based composites are also provided on Table 6. It is extremely noteworthy that the area under a stress-strain curve is a direct measurement of the energy per unit volume needed for failure of the sample and thus provides a quantitative value of the toughness. While we have not calculated these values, it is clear from the stress-strain data that for the PDMS-10,800 and PDMS-31,500 based silica composites, the toughness of the materials increase dramatically as a function of silica loading.

Results obtained from the stress-strain tests are very interesting since they indicate that the improvement in the tensile properties of the composites seem to be dependent not only on the type and amount of the silica filler, but also on the PDMS segment length in the host silicone-urea copolymer. Fig. 13 provides a plot of the tensile strength versus silica content for H2000 containing composites based on silicone-urea copolymers with different PDMS molecular weights.

For all samples, the reader will note that the tensile strengths increase linearly with silica content. Interestingly, this is similar to the trend observed in the tensile strengths of silicone-urea copolymers as a function of their urea hard segment contents [9,20].

In our earlier publications we reported a synergistic effect of the PDMS soft segment molecular weight on the tensile strength and hysteresis behavior of silicone-urea copolymers [11]. Others proposed that formation of thermodynamically stable nanocomposites is enhanced when the radius of gyration of the linear polymer is greater than the radius of the nanoparticle [21]. It is also reported that in PDMS/silica nanocomposites prepared by solution blending sections of the PDMS chains are strongly absorbed at the particle surface, forming macroscopic networks [22], which may be improved by an increase in PDMS molecular weight.

Another very interesting and informative observation made during the tensile tests was the remarkable differences in the shapes of the failed specimens, which are schematically reproduced in

Table 5
Tensile properties of PSU-3.2-7.6 and its composites based on hydrophobic (H2000) and hydrophilic (N20) silica.

Polymer Code	Silica Content (wt %)	Modulus (MPa)	Tens Str (MPa)	Elong. (%)
PSU-3.2-7.6	–	4.00	5.50	580
PSU-3.2-7.6-H-01	1.0	4.00	5.80	600
PSU-3.2-7.6-H-05	5.0	4.20	6.00	520
PSU-3.2-7.6-H-10	10	4.50	6.50	550
PSU-3.2-7.6-H-15	15	4.80	7.65	540
PSU-3.2-7.6-H-20	20	6.50	8.00	460
PSU-3.2-7.6-H-25	25	8.00	8.65	430
PSU-3.2-7.6-H-40	40	15.5	9.50	425
PSU-3.2-7.6-N-01	1.0	4.00	5.85	600
PSU-3.2-7.6-N-05	5.0	5.00	6.10	470
PSU-3.2-7.6-N-10	10	14.0	7.20	360
PSU-3.2-7.6-N-20	20	29.0	8.80	260

Table 6
Tensile properties of PSU-11-DY-5.6, PSU-32-DY-5.3 and their nanocomposites based on hydrophobic silica H2000.

Polymer Code	Silica Content (wt %)	Modulus (MPa)	Tens Str (MPa)	Elong (%)
PSU-11-DY-5.6	–	1.20	1.65	280
PSU-11-DY-5.6-H-10	10	1.40	2.50	300
PSU-11-DY-5.6-H-20	20	2.00	3.20	325
PSU-11-DY-5.6-H-40	40	4.40	4.50	480
PSU-32-DY-5.3	–	0.9	2.20	500
PSU-32-DY-5.3-H-20	20	1.2	4.15	730
PSU-32-DY-5.3-H-40	40	2.6	6.10	900
PSU-32-DY-5.3-H-60	60	5.0	7.50	880

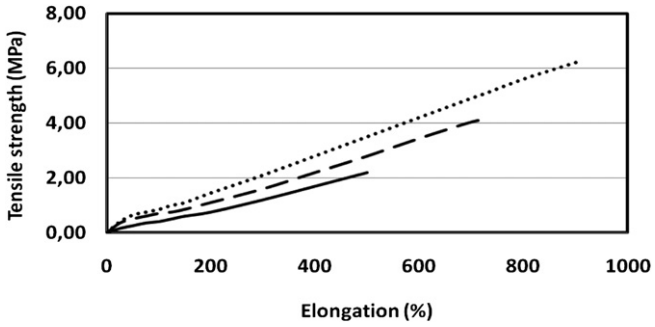

Fig. 12. Stress-strain curves for PSU-32-DY-5.3 (———), PSU-32-DY-5.3-H-20 (— — —) and PSU-32-DY-5.3-H-40 (••••••••).

Fig. 14 for the PDMS-31,500 based silicone-urea copolymer and its composites.

Unfilled silicone-urea PSU-32-DY-5.3 (Fig. 14-(a) displays a very clean fracture, typical for most elastomeric polymers. On the other hand the sample filled with 20% silica, PSU-32-DY-5.3-H-20 (Fig. 14-(b) displays a tethered rupture, while the composite containing 40% silica PSU-32-DY-5.3-H-40 (Fig. 14-(c) ruptures through almost like a diagonal tear. 60% silica containing PSU-32-DY-5.3-H-60 displays even a more complex rupture (Fig. 14-(d). Very similar rupture behaviors were also observed for PSU-3.2-7.6 and PSU-11-DY-5.6 based silica composites. In general, all the composite materials containing up to 10% by weight hydrophobic silica displayed a failure as shown in Fig. 14-(a), whereas specimens containing 20, 30 and 40% by weight silica ruptured as shown in Fig. 14-(b)–(d) respectively.

These observations clearly suggest different modes of rupture or mechanisms of failure for the composites containing different amounts of hydrophobic silica. It is also important to note from these figures that as the amount of silica in the composite increases the total area of the ruptured surface increases dramatically, which may help to promote the higher tensile strengths observed in the composites with higher silica loadings. Crack behavior and failure mechanisms of filled elastomers is rather complex and strongly dependent on a large number of parameters, which include; (i) chemical structure, size and surface properties of the filler, (ii) chemical structure and composition of the polymeric matrix, (iii) method of sample preparation and distribution of filler in the matrix, (iv) strength of filler-matrix interaction, (v) strain rate, (vi) filler content, etc. It is reported that in silica filled amorphous rubbers weak filler-matrix interface leads to better rupture properties [23,24]. The deviation in the crack propagation as a function

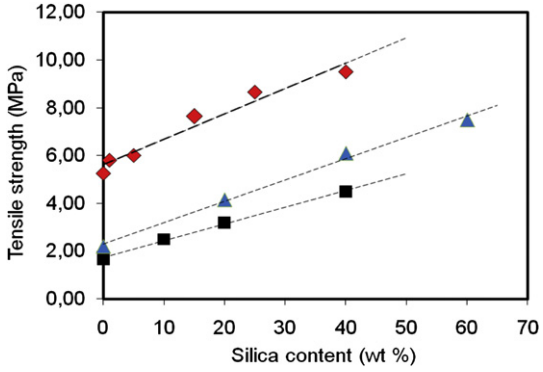

Fig. 13. Ultimate tensile strength as a function of silica (H2000) content for silicone-urea copolymers with different PDMS molecular weights. (◆) PSU-3.2-7.6, (▲) PSU-32-DY-5.3 and (■) PSU-11-DY-5.6.

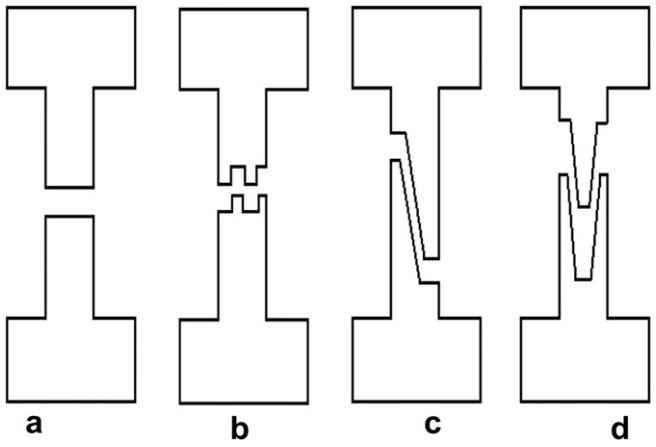

Fig. 14. Schematic description of the shapes of silica filled dog-bone specimens after failure in the tensile tests.

of silica filler may be due to changes in the crack tip geometry, leading to a reduction of the stress concentration. At larger elongations new generation of cracks may appear in the crack tip, and so on until the failure. This process would result in substantial increase in the energy needed for catastrophic failure, as observed in the silica filled PSU-32-DY-5.3 composites investigated in this study. This is a topic that may deserve further investigation in future studies.

4. Conclusions

Novel fumed silica filled segmented silicone-urea copolymer composites were prepared and characterized. The influence of silica type (hydrophilic versus hydrophobic) amount of silica loading and the PDMS soft segment molecular weight in the host copolymer on the morphology, modulus-temperature behavior and tensile properties were determined. Major observations of this study were: (i) incorporation of silica does not seem to interfere significantly with the hydrogen bonding between urea groups at room temperature, (ii) incorporation of silica does not significantly affect the glass transition or crystallization/melting behavior of PDMS, (iii) incorporation of silica significantly influences the tensile and thermomechanical properties of silicone-urea copolymers, (iv) the average molecular weight of the PDMS soft segment in the silicone-urea copolymer seem to play a significant role on the tensile properties of the composites.

Acknowledgments

The authors would like to thank Wacker Chemie for the financial support of this research. Partial financial support from the Scientific and Technical Research Council of Turkey (TUBITAK) under contact number 109M073 is also gratefully acknowledged.

References

[1] J Polym Sci Part B, Polym. Phys.. In: Manias E, Krishnamoorti R, editors. Special issue on nanocomposites, vol. 41; 2003. p. 24
[2] Koo JH. Polymer Nanocomposites: Processing, characterization and applications. New York: McGraw-Hill; 2006.
[3] Krishnamoorti R, Vaia RA. Editors, Polymer Nanocomposites: Synthesis, characterization and modeling, in: ACS Symp. Ser., 804, ACS, Washington DC, 2001.
[4] Ray SS, Bousmina M. Polymer Nanocomposites and Their Applications. New York: American Scientific Publishers; 2006.
[5] Thostenson ET, Li C, Chou TW. Compos Sci Technol 2005;65:491–516.

[6] Noll W. Chemistry and Technology of Silicones. In: Butts M, Cella J, Wood CD, Gillette G, Kerboua R, Leman J, Lewis L, Rubinsztajn S, Schattenmann F, Stein J, Wicht D, Rajaraman S, Wengrovius J, editors. Silicones. New York: Academic Press; 1968. doi:10.1002/0471238961.1909120918090308.a01.pub2. Kirk Othmer Enc. Chem. Tech.
[7] Paul DR, Mark JE. Prog Polym Sci 2010;35:893–901.
[8] Yilgor I, Sha'aban AK, Steckle Jr WP, Tyagi D, Wilkes GL, McGrath JE. Polymer 1984;25(12):1800–6.
[9] Yilgor E, Atilla GE, Ekin A, Kurt P, Yilgor I. Polymer 2003;44(26):7787–93.
[10] Tyagi D, Yilgor I, McGrath JE, Wilkes GL. Polymer 1984;25(12):1807–16.
[11] Yilgor I, Eynur T, Yilgor E, Wilkes GL. Polymer 2009;50(19):4432–7.
[12] Yilgor I, Eynur T, Bilgin S, Yilgor E, Wilkes GL. Polymer 2011;52(2):266–74.
[13] <http://www.wacker.com/cms/media/publications/downloads/6180_EN.pdf>.
[14] Yilgor I, Yilgor E, Guler GI, Ward TC, Wilkes GL. Polymer 2006;46(11):4105–14.
[15] Sheth JP, Aneja A, Wilkes GL, Yilgor E, Atilla GE, Yilgor I, et al. Polymer 2004;45(29):6919–32.
[16] Ho T, Wynne KJ, Nissan RA. Macromolecules 1993;26:7029–36.
[17] Adhikari R, Gunatillake PA, Bown MJ. Appl Polym Sci 2003;90:1565–73.
[18] Yilgor I, McGrath JE. Adv Polym Sci 1988;86:1–87.
[19] Hentschel T, Munstedt H. Polymer 2001;42(7):3195–203.
[20] Yilgor E, Yilgor I. Polymer 2001;42(19):7953–9.
[21] Mackay ME, Tuteja A, Duxbury PM, Hawker CJ, Van Horn B, Guan ZB, et al. Science 2006;311(5768):1740–3.
[22] Serbescu A, Saalwachter K. Polymer 2009;50(23):5434–42.
[23] Gherib S, Chazeau L, Pelletier JM, Satha HJ. Appl Polym Sci 2010;118:435–45.
[24] Reincke K, Grellman W, Heinrich G. Rubber Chem Technol 2004;77:662–78. doi:10.5254/1.3547843.